Journal of Alloys and Compounds 649 (2015) 380–386

Contents lists available at ScienceDirect

Journal of Alloys and Compounds

journal homepage: http://www.elsevier.com/locate/jalcom

Thermoelectric properties of *c*-$GeSb_{0.75}Te_{0.5}$ to *h*-$GeSbTe_{0.5}$ thin films through annealing treatment effects

Athorn Vora-ud [a, b, *], Mati Horprathum [c, **], Pitak Eiamchai [c], Pennapa Muthitamongkol [d], Bralee Chayasombat [d], Chanchana Thanachayanont [d], Apirak Pankiew [c], Annop Klamchuen [e], Daengdech Naenkieng [f], Theerayuth Plirdpring [f], Adul Harnwunggmoung [f], Anek Charoenphakdee [g], Weerasak Somkhunthot [h], Tosawat Seetawan [a, b, ***]

[a] Program of Physics, Faculty of Science and Technology, Sakon Nakhon Rajabhat University, Mueang District, Sakon Nakhon 47000, Thailand
[b] Thermoelectrics Research Center, Research and Development Institution, Sakon Nakhon Rajabhat University, Mueang District, Sakon Nakhon 47000, Thailand
[c] National Electronics and Computer Technology Center, National Science and Technology Development Agency, Pathumthani 12120, Thailand
[d] National Metal and Materials Technology Center, National Science and Technology Development Agency, Pathumthani 12120, Thailand
[e] National Nanotechnology Center, National Science and Technology Development Agency, Pathumthani 12120, Thailand
[f] Thermoelectric and Nanotechnology Research Center, Faculty of Science and Technology, Rajamangala University of Technology Suvarnabhumi, Huntra Phranakhon, Si Ayutthaya 13000, Thailand
[g] NANO-Thermoelectrics Research Center, Division of Applied Physics, Faculty of Sciences and Liberal Arts, Rajamangala University of Technology Isan, Mueng Nakorn Ratchasima 30000 Thailand
[h] Program of Physics, Faculty of Science and Technology, Loei Rajabhat University, Muang District, Loei 42000, Thailand

ARTICLE INFO

Article history:
Received 21 June 2015
Received in revised form
13 July 2015
Accepted 15 July 2015
Available online 17 July 2015

Keywords:
GeSbTe
Thermoelectric thin films
Pulsed dc magnetron sputtering

ABSTRACT

Germanium–Antimony–Tellurium (Ge–Sb–Te) thin films were deposited on silicon wafers with 1-μm silicon dioxide (SiO_2/Si) by pulsed dc magnetron sputtering from a 99.99% GeSbTe target of 1:1:1 ratio at ambient temperature. The samples were annealed at 573, 623, 673, and 723 K for 3600 s in a vacuum state. The effects of the annealing treatment on phase identification, atomic composition, morphology and film thickness, carrier concentration, mobility, and Seebeck coefficient of the Ge–Sb–Te samples have been investigated by grazing-incidence X-ray diffraction, auger electron spectroscopy, field-emission scanning electron microscopy, Hall-effect measurements, and steady state method, respectively. The results demonstrated that the as-deposited Ge–Sb–Te sample was amorphous. Atomic composition of as-deposited and annealed films at 573 K and 623 K were $GeSb_{0.75}Te_{0.5}$ while annealed films at 673 K and 723 K were $GeSbTe_{0.5}$ due to Sb-rich $GeSb_{0.75}Te_{0.5}$. The samples annealed at 573 K and 623 K showed the crystal phases of cubic structure (*c*-$GeSb_{0.75}Te_{0.5}$) into hexagonal structure (*h*-$GeSbTe_{0.5}$) after annealing at 673 K and 723 K. The study demonstrated the insulating condition from the as-deposited GeSbTe film, and the changes towards the thermoelectric properties from the annealing treatments. The GeSbTe films annealed at 673 K yielded excellent thermoelectric properties with the electrical resistivity, Seebeck coefficient, and power factor at approximately 1.45×10^{-5} Ωm, 71.07 μV K^{-1}, and 3.48×10^{-4} W m^{-1} K^{-2}, respectively.

* Corresponding author. Program of Physics, Faculty of Science and Technology, Sakon Nakhon Rajabhat University, Mueang District, Sakon Nakhon 47000, Thailand.
** Corresponding author. National Electronics and Computer Technology Center, National Science and Technology Development Agency, Pathumthani 12120, Thailand.
*** Corresponding author. Program of Physics, Faculty of Science and Technology, Sakon Nakhon Rajabhat University, Mueang District, Sakon Nakhon 47000, Thailand.
E-mail addresses: athornvora-ud@snru.ac.th (A. Vora-ud), mati.horprathum@nectec.or.th (M. Horprathum), t_seetawan@snru.ac.th (T. Seetawan).

http://dx.doi.org/10.1016/j.jallcom.2015.07.120
0925-8388/

1. Introduction

In modern microelectronic and photonic devices, thin-film or material coatings are important for several applications in microelectronic, electrical insulation, and sustainable energy. The sustainable energy applications, i.e., solar cells and thermoelectrics, require thin-film coatings that generate environment-friendly and clean electricity. For a clean energy production, thermoelectrics are one of the devices most recognized as promising technologies [1]. The performances of the thermoelectric materials are considered from the dimensionless figure of merit (ZT):

$$ZT = \frac{S^2 T}{\rho\kappa}, \quad (1)$$

where S, ρ, κ, and T are the Seebeck coefficient, electrical resistivity, thermal conductivity, and absolute temperature, respectively. Examples of new thermoelectric materials with high performance include the filled skutterudites [2,3], half-Heusler alloys [4], clathrate alloys [5,6], AgPbSbTe alloys [7], and GeTe–$AgSbTe_2$ alloys (TAGS) [8,9]. In 1997, Chung et al. [10] reported ternary and quaternary thermoelectric chalcogenides of long period crystal structures that yielded low thermal conductivity. In 2008 chalcogenide materials, especially those containing Ge (germanium), Sb (antimony), and Te (tellurium), are used in modern technologies due to ability to transform between two stable states, i.e., amorphous and crystalline phases [11]. The Ge–Sb–Te (GST) systems, i.e., $Ge_2Sb_2Te_5$, $GeSb_2Te_4$, and $GeSb_4Te_7$, are now being used for optical and electrical data storage because of excellent optical and electrical properties [12–14]. Sun et al. (2007) [12] reported the stacking sequence in rock salt structure of $GeSb_2Te_4$, $GeSb_4Te_7$, and $Ge_3Sb_2Te_6$ thin films compared to their lattice parameters by XRD techniques. Their experimental results are in agreement with theoretical considerations. For bulk thermoelectrics, GeSbTe is a strong candidate for high-performance thermoelectric materials, because of good electrical properties, low lattice thermal conductivity (κ_{lat}), and strong phonon scattering [15]. For thin film thermoelectrics, Lee et al. (2012) [16] reported the phase impurity and thermoelectric properties of $Ge_2Sb_2Te_5$ films deposited by DC magnetron sputtering at small thickness. In their experiments, the as-deposited $Ge_2Sb_2Te_5$ was amorphous, and became crystalline with face-centered cubic (FCC) and hexagonal close packed (HCP) phases after annealing treatments. They also used novel silicon on insulator to measure the phase and temperature, dependent Seebeck coefficients, and Thomson coefficients of $Ge_2Sb_2Te_5$ films. The Seebeck coefficient reduced from 371 $\mu V\ K^{-1}$ to 206 $\mu V\ K^{-1}$ as the crystalline fraction increased by a factor of four as quantified using X-ray diffraction. Recently, Hong and Yoon [17] reported phase change from amorphous to FCC and HCP crystalline phases, similar to ref. [16]. The variation of structures from FCC to HCP at 653 K has the highest concentration of charge carriers, the lowest electrical resistivity, and the highest power factor, respectively. Hence, the GST system has become a new material of interest for thin-film thermoelectrics and other applications within the many to compound from phase diagram [18] and electronic structure like to semi-metallic behavior [19] such as; $Ge_2Sb_2Te_5$, $GeSb_2Te_4$ and $GeSb_4Te_7$, etc. In order to prepare thin films of the chalcogenide materials, several deposition techniques can be utilized, i.e., by thermal evaporation [20], magnetron sputtering [21], pulsed laser deposition (PLD) [22], sol–gel process [23], and chemical vapor deposition (CVD) [24]. Among them, the magnetron sputtering technique has outstanding advantages, for examples, simple apparatus, high deposition rate, low deposition temperature, and large-area coating. The pulse sputtering mode of the sputtering technique, which is a focus of this study, significantly influences the particle bombardment onto the growing film on the substrate, as well as controlling the structures and compositions of the thin films [25,26].

In this work, we investigated preparation of the GeSbTe thin films by using pulsed dc magnetron sputtering system at Ge: Sb: Te of 1:1:1 ratio as a new target. The influences of the annealing temperature on structural, composition, morphological, electrical and thermoelectric properties were investigated.

2. Materials and method

2.1. Thin films preparation

The GeSbTe target (Mercantile Hi-Tech Co., Ltd.) of 0.25-inch thick and 2-inch diameters was sputtered by a magnetron sputtering system (ATC 2000-F, AJA International, Inc.) with a dc pulsed frequency of 20 kHz in high purity argon (99.999%) at ultra-high vacuum state. Substrates of SiO_2/Si in 2 × 2 cm^2 area were cleaned with acetone, isopropanol, and deionized water in an ultrasonic washer, each for 600 s, then dried in nitrogen atmosphere, and finally loaded on a substrate holder in a deposit chamber. The GeSbTe thin-film sputtering configuration was shown in Fig. 1, with the deposition conditions reported in Table 1. Set at 90 mm distance ($D_{s\text{-}t}$) from the substrate holder, the sputtering cathode was tilted at the inclined angle of 40° with respect to the substrate normal. Such inclined angles were acceptable to obtain the most optimal film uniformity. The sample was mounted on a rotating substrate plate assembly, which allowed for vertical translation (z-axis) for several inches. The substrate holder was integrated with a quartz lamp heater that allowed the annealing treatment up to 973 K. After the deposition, the as-deposited GeSbTe thin-film samples were annealed under ultra-high vacuum state at 573, 623, 673, and 723 K, each for 3600 s.

2.2. Thin films characterizations

Phase identifications of the thin films were observed by grazing-incidence X-ray diffraction (GIXRD; TTRAX III, Rigaku) operated with a Cu-$K_{\alpha 1}$ source. The measurements were conducted from 25 to 45° incident angles with a thin-film attachment mode, and then analyzed for grain size (D), lattice strain (ε), and lattice parameter. Thicknesses of the GeSbTe films were investigated by field-emission scanning electron microscopy (FE-SEM; S-4700, Hitachi). Film compositions were determined by Auger electron microscopy (AES) at 10 kV acceleration voltage, 10 nA beam current, and 40 × 40 μm^2 beam diameter. The sample surface was sputtered

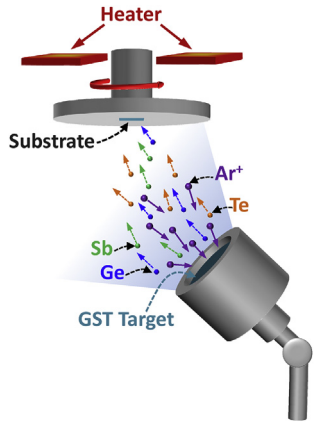

Fig. 1. Schematic of GeSbTe thin films deposition process.

Table 1
Deposition condition of GeSbTe thin films by pulsed-dc magnetron sputtering.

Base pressure (Pa)	3.2×10^{-5}
Operating pressure (Pa)	0.67
Ar flow rate (sccm)	30
DC power (W)	50
Substrate temperature (K)	RT
Deposition time (s)	3600
Substrates	SiO_2/Si wafer
Annealing temperature (K)	573, 623, 673, and 723
Annealing time (s)	3600

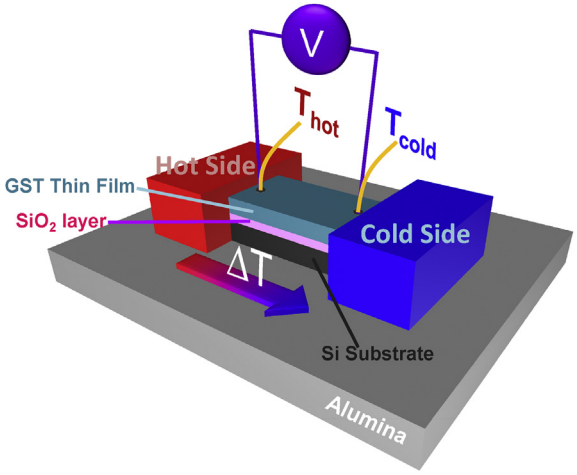

Fig. 2. Schematics of Seebeck coefficient measurement by steady state method.

for 30 s using Ar^+ ions with a fixed scan speed at 1 eV per step.

2.3. Electrical properties and Seebeck coefficient measurements

Carrier concentration and mobility in the GeSbTe thin films were measured by Hall Effect measurement system (HMS-3000, Ecopia) based on Van der Pauw four-point probe method at the room temperature. The Hall Effect measurement has been used with a large magnetic field of 0.55 T. A thin film Hall probe is placed in transverse direction of the magnetic field and adjusted current of 1–5 mA for measurements. The electrical resistivity was determined by using carrier concentration and mobility values. The Seebeck coefficient was measured by an in-house-built of a steady state method at room temperature as shown in Fig. 2. The GST thin-film samples were mounted between the copper blocks, all set up on an alumina base. These copper blocks were separately housed within heater controller to generate a temperature difference. On the surface of the samples of interest at 6.0 mm distance, temperature differences (ΔT) were monitored with k-type thermocouples to determine hot (T_{hot}) and cold (T_{cold}) temperature, while voltage differences (ΔV) were monitored with electrodes. Based on the setup, the Seebeck coefficients were measured from temperature ($\Delta T = T_{hot} - T_{cold}$) and voltage differences when heat passed through the samples from the hot to the cold side. During the measurements of the Seebeck coefficients, the temperature controller was continually adjusted to generate temperature differences in a range of 0–10 K. The values of T_{hot}, T_{cold}, and voltage were recorded from a digital multimeter (M350A, Picotest).

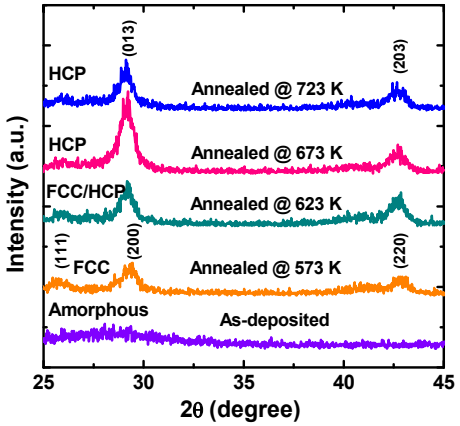

Fig. 3. XRD patterns of the as-deposit and annealed GeSbTe thin films.

3. Results and discussion

Fig. 3 shows the XRD patterns of the prepared GeSbTe thin films, which clearly exhibited phase transformation of the crystal structure. The as-deposited GeSbTe film originally showed the amorphous phase, and then seemed $Ge_2Sb_2Te_5$ cubic structure (225/Fm-3m) with (111), (200), and (220) peaks after the annealing treatment at 573 K, as confirmed by number: 054-0484 [27]. Further annealing up to 673 and 723 K seemed the $Ge_2Sb_2Te_5$ hexagonal structure (164/P-3m) with (013) and (203) peaks corresponding to number: 089-2233 [28]. The XRD intensity indicated the highest peak from the sample annealed at 673 K, and then decreased from the sample annealed at 723 K. It is noted that the annealing treatment of the sample at 623 K showed the XRD patterns that indicated a mixture between cubic structure and hexagonal structure, similar to the publications from Lee et al. (2012) [16] and Hong and Yoon (2014) [17].

In addition, from the XRD results, the annealing temperature also affected a full width at half maximum (FWHM, β), grain size (D), and lattice strain (ε) of the GeSbTe thin films. These values, including the lattice parameter, of the GeSbTe thin films were analyzed via PCXRD software Ver. 7 rel. 001 (Shimadzu) based on Debye–Scherrer's formula and Hall's method equation:

$$\beta = \left(\beta_{meas}^2 - \beta_{ref}^2\right)^{1/2}, \tag{2}$$

$$D = \frac{K\lambda}{\beta \cos\theta}, \tag{3}$$

and

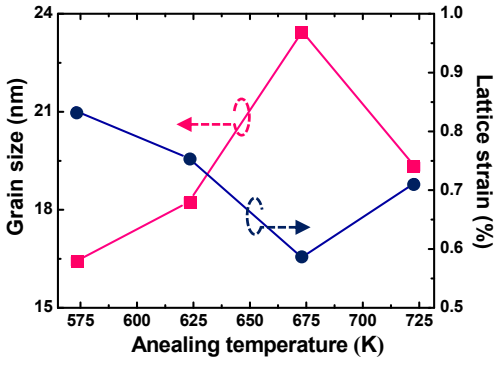

Fig. 4. The grain size and lattice strain as the function of the annealing temperature of the GeSbTe thin films.

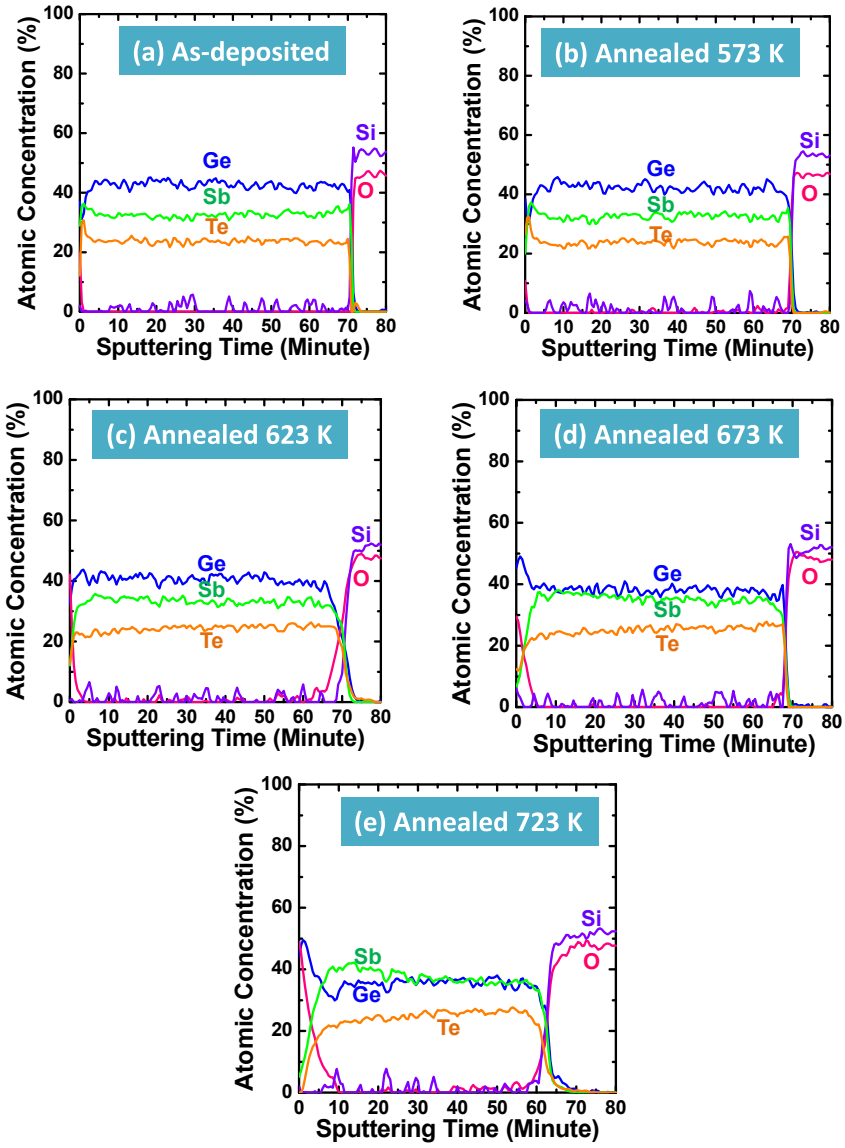

Fig. 5. The atomic concentration percentages of the GeSbTe thin films as analyzed from the AES measurements.

$$\varepsilon = \frac{\beta}{4\tan\theta}, \tag{4}$$

where β_{meas}, β_{ref}, K, λ, and θ are the measured FWHM, reference FWHM, shape factor (0.9), wavelength of CuKα radiation, and diffraction angle, respectively. The results, as shown in Fig. 4, demonstrated that the grains size of the GeSbTe films was increased with the increase in the annealing temperature from ambient condition to 673 K due to an occurrence of the crystalline structures. On the other hand, further annealing from 673 to 723 K resulted in the decrease in the grain size and the increase in the lattice strain percentage. The results, which were attributed to the thermal modification of the GeSbTe thin films and the composition variations caused by the annealing process, were confirmed with the AES measurements, as discussed in the next section.

The AES measurements for each sample were performed at five different positions on the surface, and confirmed that the compositions were uniform throughout the samples. Fig. 5 shows the compositions of the GeSbTe thin films as analyzed by the AES analyses. The results showed that the atomic concentration of the as-deposited GeSbTe thin films was approximately 44.2%, 32.3%, and 23.5% for Ge, Sb, Te, respectively, indicate that 1:0.75:0.5 for Ge:Sb:Te ($GeSb_{0.75}Te_{0.5}$ composition), which was quite different from that of the sputtering target with 1:1:1. A primary reason the as-deposited film yielded such composition was because of high plasma density, which enabled high sputtering rate of charged and neutral species from the targets [29,30]. Another crucial reason was the difference in the sputtering yields of the Ge, Sb, and Te atoms, which have been reported at approximately 0.364, 1.216, 2.063 atoms/ion at 100 eV Ar energy, or at 2.30, 6.15, and 9.91 atoms/ion at 1 keV Ar energy [31]. In our work, because the Ar energy was approximately a couple of eVs, we therefore expected a small variation in sputtering yields of the Ge, Sb, and Te elements. When the thin films were annealed at 673 K, the atomic concentrations of Ge, Sb, and Te was 38.8%, 37.3% and 23.9% respectively, which was slightly less than that in as-deposited films and indicate that 1:1:0.5 for Ge:Sb:Te. This was caused by re-evaporation of each pair of Ge, Sb, and Te elements in the GeSbTe film system during the annealing process because of different atomic bonds, as well as

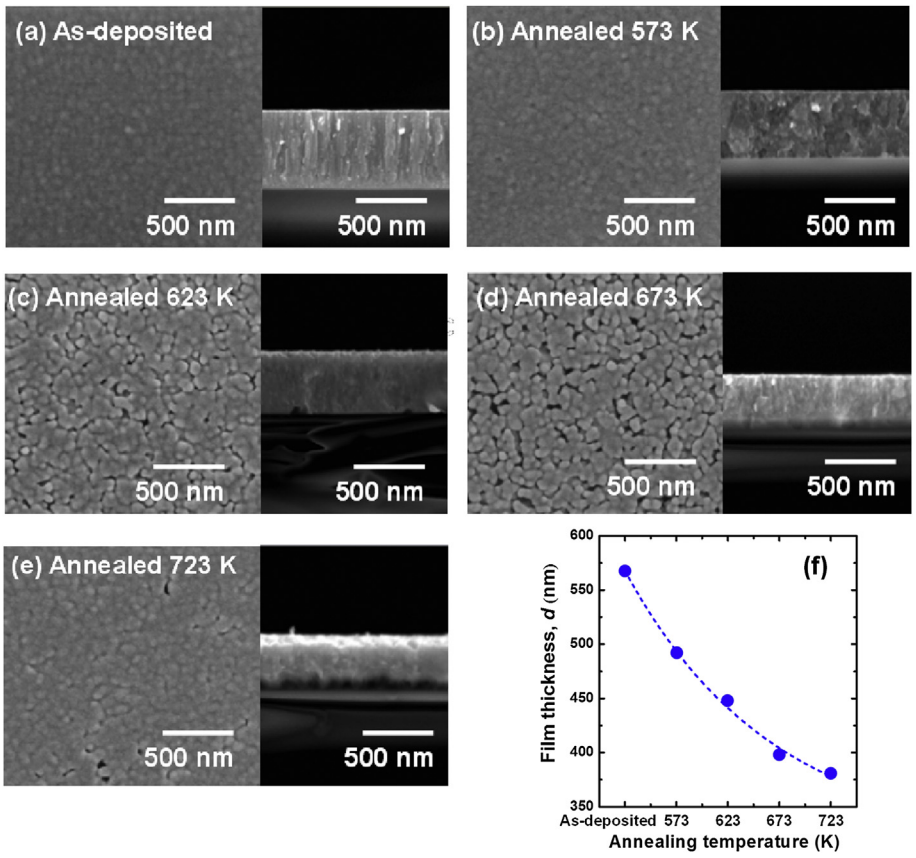

Fig. 6. (a–e) The surface and cross-sectional images of the as-deposited and annealed GeSbTe thin films. (f) The film thickness of the thin films with respect to the annealing temperature.

melting points, of the element compounds.

The surface topologies and cross sections of the films were observed by FE-SEM, as shown in Fig. 6. The as-deposited film showed a smooth surface, compact columnar structure, homogeneous morphology, and perfect adherence to the substrate. After the annealing treatment, the morphologies of the GeSbTe thin films were clearly different from that of the as-deposited sample. The annealed films showed stronger grooving features along the grain boundaries. The surface roughness was increased up to the annealing of 573 K. The annealing treatment toward 673 K caused the increase in the film roughness and grain size. Further annealing above 673 K helped smooth the surface of the film when the grain size was reduced, probably due to the suppression of crystallites on the surface. Investigations of the cross-sectional images revealed that the film thickness tended to decrease with the increase of the annealing temperature. This behavior could be explained from an insufficiency of incorporated atoms in the GeSbTe thin films at high annealing temperature, where the incorporated atoms could undergo the re-evaporation effect. This explanation had been confirmed from the AES results.

Carrier concentration and mobility values of GeSbTe thin films were measured by Hall effect method to calculate an electrical resistivity from:

$$\rho = \frac{1}{qn\mu}, \tag{5}$$

where q was carrier charge. With the above equation, we could related to $\rho = R_S d$ and $n = n_S d$, where R_S and n_S were sheet resistance and sheet carrier concentration, respectively. Hence, the

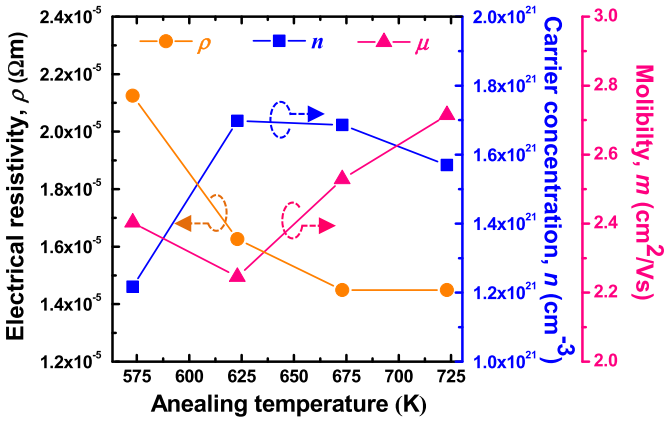

Fig. 7. Electrical resistivity, carrier concentration and mobility of annealing temperature function of the GeSbTe thin films.

sheet resistance could be determined from Eq. (6):

$$n_S = \frac{IB}{qV_H} \tag{6}$$

where V_H, I and B were Hall voltage, electric current, and magnetic field, respectively. In addition, the charge mobility could be determined from Eq. (7);

$$\mu = |V_H| R_S IB = \frac{1}{qn_S R_S} = \frac{1}{qndR_S}. \tag{7}$$

From Eq. (7), based on the relationship of carrier concentration, the charge mobility therefore depended on the film thickness and sheet resistance within the film.

The variations of the electrical resistivity, carrier concentration, and charge mobility with respect to the annealing temperature were illustrated in Fig. 7. The electrical resistivity of the GeSbTe thin films was gradually decreased from 2.12×10^{-5} Ωm to 1.44×10^{-5} Ωm with the increase in the annealing temperature. The electrical properties could be influenced by a scattering of disordered atoms, grain size, and grain boundary density in the polycrystalline structure [32]. As the annealing temperature was increased, the grain size was also increased, but the grain boundary density was instead decreased along with the decreased barrier height at the grain boundary. In addition, the results of the resistivity compared well with those from the XRD results, when the electrical resistivity changed greatly due to the phase change from the amorphous to FCC and finally to HCP structure. The decrease of the resistivity with the annealing treatment was closely related to the decrease of the lattice constant in the FCC to HCP structure [17]. However, by increasing the annealing temperature from 573 to 623 K, the carrier concentration was increased and the mobility was decreased because of the reduction of the anti-structural defects. However, when the annealing temperature was increased from 623 to 723 K, the carrier concentration was now decreased and the mobility was increased because of the grain growth. Note that, although the values of the electrical resistivity, carrier concentration, and charge mobility varied slightly with respect to the annealing temperature, these values were not measureable from the as-deposited sample at all. The annealing treatment therefore greatly affects the as-deposited GeSbTe thin-film system, whose Seebeck coefficients and power factors would be further discussed in the next section.

Seebeck coefficient of GeSbTe thin films was measured by using steady state method based on the electromotive force (EMF). With an open circuit voltage and no current flow, the Seebeck coefficients were determined from:

$$S = \frac{\Delta V}{\Delta T}, \tag{8}$$

where ΔV and ΔT were the electrical voltage and temperature differences, respectively. In theoretical term, the Seebeck coefficient has been related to carrier concentration and mobility to be limited in power factor [33], as follows:

$$P = \frac{S^2}{\rho}. \tag{9}$$

The effects of the annealing temperature to the thermoelectric properties of the GeSbTe thin films were shown in Fig. 8(a). It can be seen that both the Seebeck coefficient and the power factor were increased with increased annealing temperature up to 673 K. The results were attributed from the increase in the electrical conductivity because of the elimination of defects, the growth of grain, and the decreased scattering of carrier. However, at 723 K annealing treatment, both thermoelectric properties of the GeSbTe film was suddenly decreased when the film thickness and the film composition changed, as already discussed in the FE-SEM and AES analyses. In order to investigate the performance of the prepared GeSbTe thin films, the authors compared the experimental data with reference data of (25 nm-thick) $Ge_2Sb_2Te_5$ ultra-thin film [16] and (500 nm) $Ge_2Sb_2Te_5$ thick film [17], as shown in Fig. 8(b) and (c). Both sets of the reference also included the variation of the

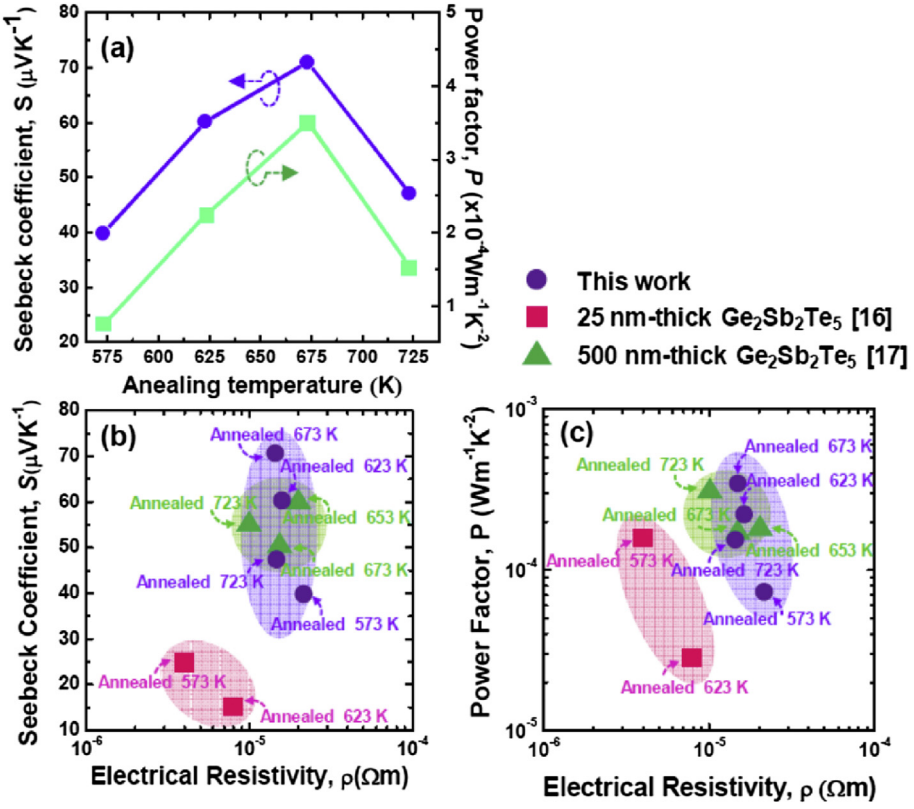

Fig. 8. (a) The Seebeck coefficient and the power factor with respect to the annealing temperature of the GeSbTe thin films. (b and c) The zone diagrams of the Seebeck coefficient and the power factor with respect to the electrical resistivity, in comparison with notable published results.

annealing temperature, from which the electrical resistivity ranged from 10^{-6} to 10^{-4} Ωm. From the figures, our prepared GeSbTe thin films yielded slightly higher Seebeck coefficients, and nearly identical power factors, within the same range of the electrical resistivity of the reference $Ge_2Sb_2Te_5$ thick films. For the reference $Ge_2Sb_2Te_5$ ultra-thin films, their values of the electrical resistivity were generally smaller, but more reliable to smaller thermoelectrics. Note that, our annealed GeSbTe films at 673 K with 397 nm final film thickness yielded the Seebeck coefficient of 71.07 μV K^{-1} and the power factor of 3.49×10^{-4} W m^{-1} K^{-2}, which were both higher than those of the reference 500 nm $Ge_2Sb_2Te_5$ film. It could be explained that the compositions of the prepared GeSbTe films, especially for the Sb element, changed with the annealing treatments, as already observed from in AES results. With the annealing process, the Sb-rich GeSbTe films were obtained as a correlation to the disorder induced by localization of the charge carriers. Such Sb-rich films therefore could have larger effective carrier concentration (1.68×10^{21} cm^{-3}) which was higher than that of the reference 500 nm $Ge_2Sb_2Te_5$ film (10^{20} cm^{-3}).

4. Conclusion

The GeSbTe thin films were deposited on the silicon wafers with 1-μm silicon dioxide by pulsed dc magnetron sputtering. The prepared thin films were annealed at 573, 623, 673, and 723 K for 1 h in a vacuum state. The effects of the annealing treatment were investigated based on crystal structures, physical morphologies, atomic compositions, and the thermoelectric properties of the GeSbTe samples. The results demonstrated the phase transformations of the films' crystal structures from the amorphous to the cubic, and finally to the hexagonal. The electrical resistivity of GeSbTe thin film was decreased with increasing annealing treatment temperature. At the annealing temperature of 673 K, the GeSbTe sample demonstrated the lowest electrical resistivity at 1.45×10^{-5} Ωm. In addition, the annealed sample also indicated the highest Seebeck coefficient at the power factor at 71.07 μV K^{-1}, and 3.48×10^{-4} W m^{-1} K^{-2}, respectively.

Acknowledgments

Financial supported by “Thailand Research Fund (TRF) through the Royal Golden Jubilee (RGJ) Ph.D. Program (Grant No. PHD/0126/2556)” is acknowledged. The authors would also express high gratitude toward the Optical Thin-Film Technology Laboratory (OTL), National Electronics and Computer Technology Center (NECTEC) and Thai Thermoelectric Society, Thailand for the deposition facilities and Physical Characterization Laboratory (PHCL), National Metal and Materials Technology Center (MTEC), Thailand for the characterization equipments.

References

[1] F. Yan, T.J. Zhu, X. Zhao, Appl. Phys. A 88 (2007) 425.
[2] G.S. Nolas, M. Kaeser, R.T. Littleton, T.M. Tritt, Appl. Phys. Lett. 12 (2000) 1855.
[3] B.C. Chakoumakos, B.C. Sales, J. Alloys Compd. 87 (2006) 407.
[4] K. Mastronardi, D. Young, C.C. Wang, P. Khalifah, R.J. Cava, A.P. Ramirez, Appl. Phys. Lett. 74 (1999) 1415.
[5] A. Bentien, M. Christensen, J.D. Bryan, A. Sanchez, S. Paschen, F. Steglich, G.D. Stucky, B.B. Iversen, Phys. Rev. B 69 (2004) 1.
[6] N.P. Blake, L. Mollnite, G. Kresse, H. Metiu, J. Chem. Phys. 111 (1999) 3133.
[7] K.F. Hsu, S. Loo, F. Guo, W. Chen, J.S. Dyck, C. Uher, T. Hogan, E.K. Polychroniadis, M.G. Kanatzidis, Science 303 (2004) 818.
[8] J.W. Sharp, in: Proc. 22nd Int. Conf. on Thermoelectrics, 2003, p. 267.
[9] L.A. Flanders, R.W. Drinker, B. Heshmatpour, D.S. Moul, J.P. Fleurial, K.L. Tuttle, Space Technol. Apps. Internat. Forum – STAIF (2005) 564.
[10] D.K. Chung, T. Hogan, J. Schindler, L. Iordanidis, P. Brazis, C.R. Kan-newurf, B.X. Chen, C. Uher, M.G. Kanatzidis, in: Proc. XVI Int. Conf. Thermoelectrics, 1997, p. 459.
[11] A.A. Bahgat, A.S. AbdRabo, I.A. Mahdy, E.P. Domashevskaya, Opt. Laser. Technol. 40 (2008) 1061.
[12] Z. Sun, S. Kyrsta, D. Music, R. Ahuja, J.M. Schneider, Solid State Commun. 143 (2007) 240.
[13] N. Yamada, E. Ohno, K. Nishiuchi, N. Akahira, M. Takao, J. Appl. Phys. 69 (1991) 2849.
[14] A.V. Kolobov, P. Fonf, A.I. Frenkel, A.L. Ankudinov, J. Tominga, T. Uruga, Nat. Mater. 3 (2004) 703.
[15] A. Kosuga, K. Nakai, M. Matsuzawa, Y. Fujii, R. Funahashi, T. Tachizawa, Y. Kubota, K. Kifune, J. Alloys Compd. 618 (2015) 463.
[16] J. Lee, T. Kodama, Y. Won, M. Asheghi, K.E. Goodson, J. Appl. Phys. 112 (2012) 014902.
[17] J.E. Hong, S.G. Yoon, ECS J. Solid State Sci. Technol. 3 (10) (2014) 298.
[18] N.P. Reddy, C. Bapanayya, R. Gupta, S.C. Agarwal, Pramana J. Phys. 80 (6) (2013) 1065.
[19] A. Vora-Ud, W. Somkhunthot, T. Seetawan, Integr. Ferroelectr. 155 (2014) 52.
[20] D.A.P. Bulla, R.P. Wang, A. Prasad, A.V. Rode, S.J. Madden, B. Luther-Davies, Appl. Phys. A Mater. Sci. Process. 96 (2009) 615.
[21] W.C. Tan, M.E. Solmaz, J. Gardner, R. Atkins, C. Madsen, J. Appl. Phys. 107 (2010) 033524.
[22] R.K. Pan, H.Z. Tao, H.C. Zang, C.G. Lin, T.J. Zhang, X.J. Zhao, J. Non-Cryst. Solids 357 (2011) 2358.
[23] M. Krbal, T. Wagner, T. Kohoutek, P. Nemec, J. Orava, M. Frumar, J. Phys. Chem. Solids 68 (2007) 953.
[24] C.C. Huang, D.W. Hewak, J.V. Badding, Opt. Express 12 (2004) 2501.
[25] W. Somkhunthot, T. Burinprakhon, I. Thomas, T. Seetawan, V. Amornkitbamrung, Elektrika 9 (2) (2007) 20.
[26] M. Horprathum, P. Eiamchai, P. Chindaudom, N. Nuntawong, V. Patthanasettakul, P. Limnonthakul, P. Limsuwan, Thin Solid Films 520 (2011) 272.
[27] T. Matsunaga, N. Yamada, Jpn. J. Appl. Phys. 41 (2002) 1674.
[28] I.I. Petrov, R.M. Imamov, Z.G. Pinsker, Kristallografiya 13 (1968) 417.
[29] M. Kumar, L. Wen, B.B. Sahu, J.G. Han, Appl. Phys. Lett. 106 (2015) 241903.
[30] M. Kumar, T. Kumar, D.K. Avasthi, Scr. Mater 105 (2015) 46.
[31] http://www.npl.co.uk/science-technology/surface-and-nanoanalysis/services/sputter-yield-values.
[32] Z. Zeng, P. Yanga, Z. Hua, Appl. Surf. Sci. 268 (2013) 472.
[33] H. Alam, S. Ramakrishna, Nano Energy 2 (2013) 190.